



# CHEMISTRY

## A European Journal



### Accepted Article

**Title:** Intersystem Crossing in Naphthalenediimide-Oxoverdazyl Dyads: Synthesis and Study of the Photophysical Properties

**Authors:** Mushraf Hussain, Maria Taddei, Laura Bussotti, Paolo Foggi, Jianzhang Zhao, Qingyun Liu, and Mariangela Di Donato

This manuscript has been accepted after peer review and appears as an Accepted Article online prior to editing, proofing, and formal publication of the final Version of Record (VoR). This work is currently citable by using the Digital Object Identifier (DOI) given below. The VoR will be published online in Early View as soon as possible and may be different to this Accepted Article as a result of editing. Readers should obtain the VoR from the journal website shown below when it is published to ensure accuracy of information. The authors are responsible for the content of this Accepted Article.

**To be cited as:** *Chem. Eur. J.* 10.1002/chem.201903814

**Link to VoR:** <http://dx.doi.org/10.1002/chem.201903814>

Supported by  
**ACES**

WILEY-VCH

# Intersystem Crossing in Naphthalenediimide-Oxoverdazyl Dyads: Synthesis and Study of the Photophysical Properties

Mushraf Hussain,<sup>[a]</sup> Maria Taddei,<sup>[b]</sup> Laura Bussotti,<sup>[b]</sup> Paolo Foggi,<sup>[b][c][d]</sup> Jianzhang Zhao<sup>\*[a]</sup> Qingyun Liu,<sup>\*[e]</sup> and Mariangela Di Donato<sup>\*[b][c]</sup>

**Abstract:** Oxoverdazyl (Vz) radical units were covalently linked to naphthalenediimide (NDI) chromophore to study the effect of radical on the photophysical properties, especially the radical enhanced intersystem crossing (REISC), which is a promising approach to develop heavy atom-free triplet photosensitizers. Rigid phenyl or ethynylphenyl linkers between the two moieties were used, thus REISC and formation of doublet (total spin quantum number  $S = 1/2$ ) and quartet states ( $S = 3/2$ ) are anticipated. The photophysical properties of the dyads were studied with steady state and femtosecond/nanosecond transient absorption (TA) spectroscopies and density functional theory (DFT) computations. Femtosecond transient absorption spectra show a fast electron transfer (<150 fs), and ISC (ca. 1.4 ~ 1.85 ps) is induced by charge recombination (CR). In toluene. Nanosecond transient absorption spectra demonstrated a biexponential decay of the triplet state of the NDI moiety. We assign the fast component (lifetime: 50 ns; population ratio: 80%) to the  $D_1 \rightarrow D_0$  decay, and the slow decay component (2.0  $\mu$ s; 20%) to the  $Q_1 \rightarrow D_0$  ISC. DFT computations indicated ferromagnetic interactions between radical and chromophore ( $J = 0.07$  eV ~ 0.13 eV). Reversible formation of the radical anion of NDI moiety by photoreduction of the radical-NDI dyads in the presence of sacrificial electron donor triethanolamine (TEOA) is achieved. This work is useful for design of new triplet photosensitizer based on REISC effect.

## Introduction

Triplet photosensitizers are compounds showing strong

absorption of UV/vis light, efficient intersystem crossing (ISC),<sup>[1]</sup> and long-lived triplet excited states.<sup>[2]</sup> These compounds can be used in photodynamic therapy (PDT),<sup>[3,4]</sup> photocatalysis,<sup>[5-7]</sup> and triplet-triplet annihilation (TTA) upconversion.<sup>[1,3,4]</sup> Different methods are used to enhance the ISC, including the heavy atom effect,<sup>[5]</sup> hyperfine coupling,<sup>[6,7]</sup> exciton coupling,<sup>[5]</sup> and the use of spin converters.<sup>[5]</sup>

The use of radicals to enhance ISC is of particular interest, and is often referred as radical enhanced ISC (REISC).<sup>[8,9]</sup> The REISC mechanism is based on the spin-spin exchange of the electrons localized on the radical and on the electronically excited chromophore. With spin-spin interaction between the radical and the electronically excited chromophore, the three spin system may form a doublet state (D, total spin quantum number  $S = 1/2$ ) or a quartet state (Q, total spin quantum number  $S = 3/2$ ). The formation of the doublet spin state is beneficial for ISC: the ISC of the chromophore is within the overall  $D_n \rightarrow D_1$  transition of the dyad, which is a spin allowed process (herein for  $D_n$  state, the chromophore in singlet state; for  $D_1$  state, the chromophore is in triplet state).<sup>[9,10]</sup> Previously, radical labeled fluorophores were mainly used as fluorescent molecular probes for selective detection of reactive radicals,<sup>[8,11-14]</sup> based on the quenching of fluorescence by the attached radical on the fluorophore, and fluorescence recovery of the fluorophore upon reaction of the radical with the analytes. However, the quenching mechanisms of the radical on the fluorescence were not studied in detail.<sup>[12]</sup> Actually, in most of these systems, electron spin alignment at the electronic excited state was observed, leading to the formation of doublet, quartet and quintet states for the mono and biradical-labeled chromophores. The electron spin dynamics of these molecular systems were characterized with time-resolved electron paramagnetic resonance (TREPR) spectroscopy.<sup>[8,15,16]</sup> However, little attention has been devoted to characterize the chromophore localized triplet formation in these systems in terms of triplet photosensitizers.<sup>[9,17]</sup> Moreover, only a limited number of chromophores have been used in EISC, for instance naphthalene,<sup>[18]</sup> anthracene,<sup>[19]</sup> perylene,<sup>[20]</sup> pyrene,<sup>[21,22]</sup> perylenebisimide<sup>[23,24]</sup> and Bodipy.<sup>[9]</sup> There are rare reports concerning other chromophores showing strong absorption of visible light, such as naphthalenediimide (NDI), for studying of REISC.

In the previously studied molecular systems, the radical and the chromophores were either mechanically mixed,<sup>[8,25-27]</sup> or covalently linked via saturated bonds.<sup>[28]</sup> These strategies usually induced weak electron spin-spin exchange interaction between the radical and the electronically excited chromophore. To the best of our knowledge,  $\pi$ -conjugated linkers between the radical and chromophore units were rarely studied. A nitroxide radical-anthracene compound was reported but the  $\pi$ -conjugation between the radical and the chromophore is doubtful, since the two moieties may adopt an orthogonal orientation.<sup>[27]</sup> It is proposed that the spin-spin exchange is

[a] M. Hussain, Prof. J. Zhao  
State Key Laboratory of Fine Chemicals, School of Chemical Engineering, Dalian University of Technology, E-208 West Campus, 2 LingGong Road, Dalian 116024, P. R. China.  
E-mail: zhaojzh@dlut.edu.cn

[b] M. Taddei, Dr. L. Bussotti, Prof. P. Foggi, Dr. M. D. Donato  
LENS (European Laboratory for Non-Linear Spectroscopy), Via N. Carrara 1, 50019 Sesto Fiorentino, Italy.

[c] Prof. P. Foggi, Dr. M. D. Donato  
D INO, Istituto Nazionale di Ottica Largo Enrico, Fermi 6, I-50125 Florence, Italy.  
E-mail: didonato@lens.unifi.it

[d] Prof. P. Foggi,  
Dipartimento di Chimica, Università di Perugia, via Elce di Sotto 8, 06123 Perugia, Italy

[e] Prof. Qingyun Liu  
College of Chemical and Environmental Engineering, Shandong University of Science and Technology, Qingdao, 266590, P. R. China  
E-mail: qyliu@sdust.edu.cn

Supporting information for this article is given via a link at the end of the document.

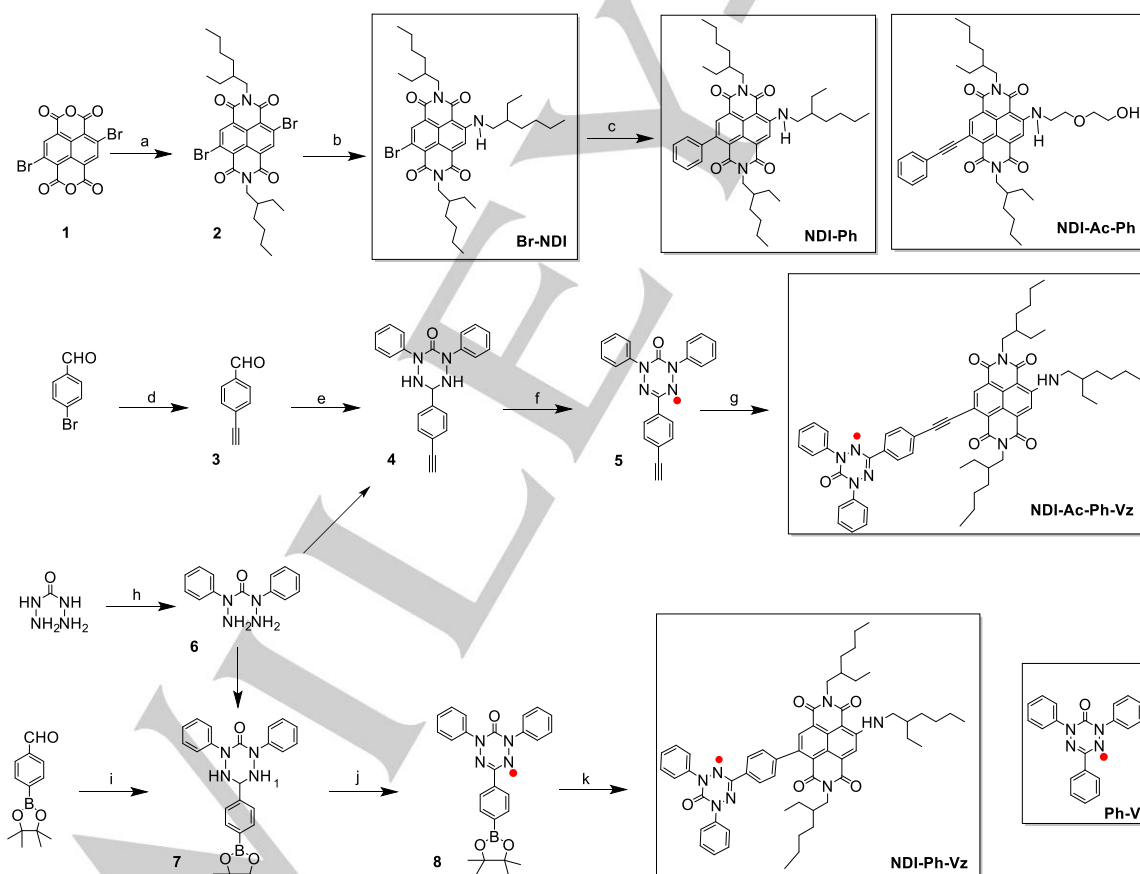
strong, although the  $J$  value was not determined experimentally or theoretically.<sup>[28]</sup> Verdazyl radical was directly connected to a pyrene moiety, formation of quartet state was characterized with TREPR.<sup>[21]</sup> However, the effect of the radical on the photophysical properties of the chromophore is elusive. For instance, it has been found that in a Ru(II) trisbipyridine complex, the triplet state of the coordination center was not affected by the attached verdazyl ligand.<sup>[29]</sup> It was found that the singlet excited state of pentacene was not quenched by the attached TEMPO radical (a stable nitroxide radical).<sup>[30]</sup> In most cases, the formation of the high spin states (doublet, quartet or quintet states) was studied with the TREPR, but the kinetics of their formation and decay have been rarely characterized using nanosecond and femtosecond transient absorption spectroscopy. Herein we prepared two NDI-Vz dyads (**NDI-Ac-Ph-Vz** and **NDI-Ph-Vz**, Scheme 1); different  $\pi$ -conjugated linkers were used to connect the two units. The fixed distance and orientation between the radical and the chromophore is beneficial for the formation of D (spin angular momentum quantum number  $S = 1/2$ ) and Q states (spin angular momentum quantum number  $S = 3/2$ ).<sup>[8,24]</sup> Based on steady state and time-resolved transient absorption spectroscopies, the photo-induced electron transfer

and the charge recombination-induced ISC kinetics of NDI chromophore were studied. DFT computations indicated ferromagnetic spin-spin coupling between the radical and the NDI chromophore.

## Results and Discussion

### Design and synthesis of the dyads

In **NDI-Ac-Ph-Vz** and **NDI-Ph-Vz** (Scheme 1), rigid linkers were used to connect the radical and the NDI chromophores, because fixed distance and orientation of the two moieties are beneficial for the formation of high spin states, as such the modulation of the photophysical property of the chromophore is expected.<sup>[8,24]</sup> Differently from the previously reported chromophore-radical molecular systems, in these two new dyads (Scheme 1), the chromophore and radical moieties are linked through unsaturated bonds to increase the  $\pi$ -conjugation.<sup>[24]</sup> According to the topology rule for the spin alignment, the spin-spin exchange between the radical and the NDI triplet in both dyads will be *ferromagnetic* ( $J > 0$ ).<sup>[31–33]</sup> **NDI-Ph**, **NDI-Ac-Ph**, **Br-NDI** and **Ph-Vz** were prepared as reference compounds.



**Scheme 1.** Synthesis of NDI-verdazyl dyads. <sup>a</sup> Key: (a) 2-Ethylhexylamine, acetic acid, stirred for 2 h, Ar, 120 °C, Yield: 32 %; (b) 2-Ethylhexyl amine, refluxed for 5 h, Ar, 120 °C, Yield: 72 %; (c) Phenyl boronic acid, K<sub>2</sub>CO<sub>3</sub>, Pd(PPh<sub>3</sub>)<sub>4</sub>/CuI, acetone/water, refluxed for 8 h, Ar, 90 °C, Yield: 94 %; (d) (i) 4-Bromobenzaldehyde, Trimethylsilyl acetylene (TMS), Pd(PPh<sub>3</sub>)<sub>4</sub>Cl<sub>2</sub>/PPh<sub>3</sub>/CuI, Et<sub>3</sub>N, refluxed for 8 h, Ar, 90 °C; (ii) K<sub>2</sub>CO<sub>3</sub>, MeOH, stirred for 0.5 h, Ar, 25 °C, Yield: 65 %; (e) Pyridinium toluene-4-sulphonate, CH<sub>3</sub>OH, stirred for 0.5 h, Ar, 25 °C, Yield: 70 %; (f) Benzoquinone, toluene, refluxed for 0.5 h, 90 °C, Yield: 86 %; (g) Pd(PPh<sub>3</sub>)<sub>4</sub>/CuI, toluene, diisopropyl amine, stirred for 18 h, 80 °C, Yield: 51 %; (h) CuI, Iodobenzene, K<sub>3</sub>PO<sub>4</sub>, phenanthroline, DMF, 28 h, Ar, 90 °C, Yield: 36 %; (i) Pyridinium toluene-4-sulphonate, C<sub>2</sub>H<sub>5</sub>OH, 12 h, Ar, 80 °C, Yield 76 %; (j) *p*-benzoquinone, toluene, 1.5 h, 90 °C, Yield: 63 %; (k) K<sub>2</sub>CO<sub>3</sub>, Pd(OAc)<sub>2</sub>, acetone, water, 2 h, 60 °C, Yield: 43 %.

Suzuki-Miyaura cross coupling reaction was used for the synthesis of **NDI-Ph** and **NDI-Ph-Vz** (Scheme 1). **NDI-Ac-Ph** and **NDI-Ac-Ph-Vz** were synthesized by Pd(0) catalyzed Sonogashira cross coupling reaction. All the compounds were isolated in moderate to satisfactory yields (see Experimental sections). It should be noted that no satisfactory  $^1\text{H}$  NMR spectra can be recorded for the radical compounds (paramagnetic). The molecular structures were verified by HRMS, FTIR, ESR and elemental analysis.

### UV-Vis absorption and fluorescence emission spectra

**NDI-Ph-Vz** shows a strong absorption centered at 535 nm with a shoulder at 580 nm (Figure 1a). The peak at 535 nm is the absorption of the  $\pi-\pi^*$  transition of NDI moiety, which was also observed for **NDI-Ph**. The shoulder absorption at 580 nm is due to the verdazyl moiety, but the intensity at this wavelength is higher as compared to the absorption of the reference **Ph-Vz**, suggesting the occurrence of some interaction between the two moieties in **NDI-Ph-Vz**. This assumption is further supported by the absorption band of **NDI-Ph-Vz** centered at 300 nm, which almost doubles in intensity as compared to **NDI-Ph**. **NDI-Ac-Ph-Vz** has an intense absorption band centered at 550 nm, which is 15 nm red shifted as compared to **NDI-Ph-Vz** (Figure 1b), the shoulder absorption band at 580 nm is due to the verdazyl unit. The structure of **NDI-Ac-Ph-Vz** is coplanar between the radical and the NDI units (see computational section), therefore, in order to study the stacking effect, we compared the UV-vis spectra of the compound in different solvents (Supporting information, Figure S23), however, no significant difference was observed. We also recorded UV-vis spectra by increasing the concentration of **NDI-Ac-Ph-Vz**, but no shifting of peaks was observed (Supporting information, Figure S24). These results indicate that there is no stacking effect for the radical compound. Upon the introduction of the verdazyl moiety in **NDI-Ph-Vz** (535 nm) and **NDI-Ac-Ph-Vz** (550 nm), the absorption band of the NDI moiety is red shifted by approximately 5 nm as compared to the references **NDI-Ph** (530 nm) and **NDI-Ac-Ph** (545 nm).

No significant difference in absorbance in solvents with different polarity (Supporting information, Figure S23). The UV-vis absorption spectra of **NDI-Ph-Vz**, **NDI-Ac-Ph-Vz**, **NDI-Ph** and **NDI-Ac-Ph** are compared with their calculated absorption spectra (Figure 2; Supporting Information, Figure S25 and S26).

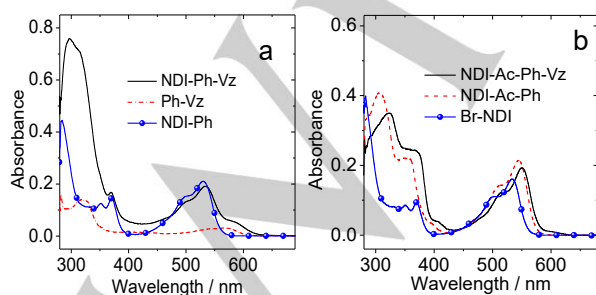


**Figure 1.** UV-vis absorption spectra of (a) **NDI-Ph-Vz**, **Ph-Vz**, **NDI-Ph** and (b) **NDI-Ac-Ph-Vz**, **NDI-Ac-Ph**, **Br-NDI**.  $c = 1.0 \times 10^{-5}$  M in toluene, 20 °C.

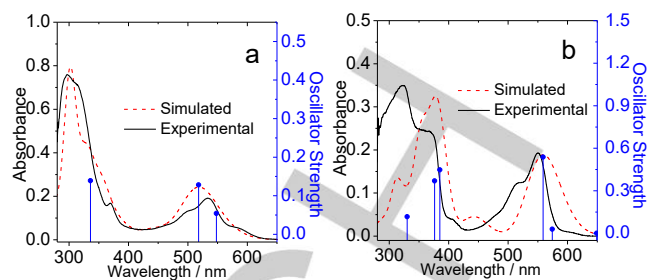


**Figure 2.** Comparison of experimental and simulated UV-vis absorption spectra of (a) **NDI-Ph-Vz** (b) **NDI-Ac-Ph-Vz** in toluene. Drop lines indicate the oscillator strength of the calculated spectra at specific wavelength. Computed at UB3LYP/6-31G(d) level using Gaussian 09W.

The computed absorption spectra are obtained by TDDFT calculations performed at UB3LYP/6-31G(d), UB3LYP/6-31G+(d) for radical and B3LYP/6-31G(d) levels for reference compounds respectively with Gaussian 09W.<sup>[34]</sup> UB3LYP/6-31G(d) was found to be better for **NDI-Ac-Ph-Vz** and almost similar for **NDI-Ph-Vz** (Supporting Information, Figure S25). For **NDI-Ph-Vz**, the calculated absorption band is at 549 nm, which is close to the experimental absorption band at 535 nm. This transition is mainly localized on the NDI moiety with a minor contribution from the radical unit. Similarly, a transition at 517 nm is also localized on the NDI moiety with a little contribution from the verdazyl unit. A strong absorption band in the 300–350 nm region was also predicted by computations, due to an electronic transition between radical and chromophore, and it is with partially CT character, based on the molecular orbitals involved in the transition (Supporting Information, Figure S37).

For **NDI-Ac-Ph-Vz**, the calculated absorption band is at 559 nm, in agreement with the experimentally observed absorption band at 549 nm. TDDFT results indicated that this transition is localized on the NDI moiety. A strong absorption band at 386 nm was also observed for **NDI-Ac-Ph-Vz**. The molecular orbitals show that this transition is mainly confined on the verdazyl unit, with minor contribution from the NDI moiety. For both radicals the transition obtained for wavelength longer than 550 nm are partially localized on the Vz moiety, indicating that there is absorption due to radical.

**NDI-Ph**, **NDI-Ac-Ph** and **Br-NDI** show strong emission bands centered at 570 nm, 563 nm and 559 nm, respectively (Figure 3a and Table 1). The fluorescence quantum yields ( $\Phi_F$ ) were determined as 80%, 29% and 23% for **NDI-Ph**, **NDI-Ac-Ph** and **Br-NDI**, respectively (Table 1). However, for **NDI-Vz** dyads, the emission is drastically quenched (Figure 3b). For instance, **NDI-Ph-Vz** has a very weak emission band centered at 558 nm. The fluorescence quantum yield of **NDI-Ph-Vz** is only 0.7%, much less as compared to **NDI-Ph** ( $\Phi_F = 80\%$ , Table 1). The emission maximum of **NDI-Ac-Ph-Vz** is at 576 nm, which is slightly red shifted as compared to **NDI-Ac-Ph** (Figure 3b). The fluorescence quantum yield is very low (0.3%).

The solvatochromic behavior of the dyads is almost similar to that of the non-radical compounds (Supporting Information, Figure S27). Both radicals and non-radical compounds show a similar quenching trend going from non-polar to polar solvents.

**Table 1.** Photophysical parameters of the compounds<sup>[a]</sup>

	$\lambda_{\text{abs}}$ / nm <sup>[a]</sup>	$\epsilon$ <sup>[b]</sup>	$\lambda_{\text{em}}$ <sup>[a]</sup>	$\Phi_{\text{F}}$ <sup>[c]</sup> / %	$\tau_{\text{F}}$ <sup>[d]</sup> / ns	$\Phi_{\Delta}$ <sup>[e]</sup> / %	$\tau_{\text{T}}$ <sup>[f]</sup> / $\mu\text{s}$
<b>NDI-Ph-Vz</b>	535	1.9	558	0.7	9.6	26 <sup>[g]</sup> , 2 <sup>[h]</sup> , $\text{--}$ <sup>[i,j]</sup>	1.9, 0.06
<b>NDI-Ac-Ph-Vz</b>	550	1.9	576	0.3	8.9	24 <sup>[g]</sup> , 6 <sup>[h]</sup> , $\text{--}$ <sup>[i,j]</sup>	2.5, 0.05
<b>NDI-Ph</b>	530	2.1	563	80	10.6	18 <sup>[g]</sup> , 16 <sup>[h]</sup> , 15 <sup>[i]</sup>	114.4
<b>NDI-Ac-Ph</b>	545	2.1	570	29	10.3	12 <sup>[g]</sup> , 10 <sup>[h]</sup> , 9 <sup>[i]</sup>	78.2
<b>Br-NDI</b>	534	1.6	559	23	4.9	76 <sup>[g]</sup> , 62 <sup>[h]</sup> , 75 <sup>[i]</sup>	42.3
<b>Ph-Vz</b>	575	0.3	$\text{--}$ <sup>[k]</sup>	$\text{--}$ <sup>[k]</sup>	$\text{--}$ <sup>[k]</sup>	$\text{--}$ <sup>[k]</sup>	$\text{--}$ <sup>[k]</sup>

[a] In toluene ( $1.0 \times 10^{-5}$  M), in nm. [b] Molar absorption coefficient.  $\epsilon$ :  $10^4 \text{ M}^{-1} \text{ cm}^{-1}$ . [c] Fluorescence quantum yield with Diiodo-Bodipy used as standard ( $\Phi_{\text{F}} = 2.9\%$  in  $\text{CH}_2\text{Cl}_2$ ), [d] Fluorescence lifetime. [e] Singlet Oxygen quantum yields ( $\Phi_{\Delta}$ ). Excited at  $\lambda_{\text{exc}} = 525$  nm, Diiodo-Bodipy was used as standard ( $\Phi_{\Delta} = 85.0\%$  in toluene). [f] Triplet state lifetime measured by nanosecond transient absorption spectra. [g] In toluene. [h] In  $\text{CH}_3\text{CN}$ . [i] In *n*-hexane, [j] Not detected, [k] Not applicable.

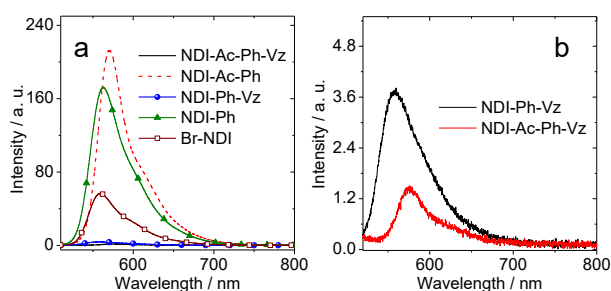


**Figure 3.** Fluorescence emission spectra of (a) all the compounds (b) NDI-Vz radicals ( $\lambda_{\text{ex}} = 500$  nm); optically matched solutions were used.  $c = \text{ca. } 1.0 \times 10^{-5}$  M in toluene. 20 °C.

The quenching of the NDI fluorescence in the radical-containing dyads can be due to electron spin-spin exchange, charge separation, thermal relaxation or solvent shell relaxation. However, photo-induced electron transfer (PET) is also possible to reduce the emission,<sup>[35,36]</sup> supported by cyclovoltammetric studies (See later section). Radical enhanced internal conversion may also play a role in the overall quenching process. In order to exclude the *intermolecular* quenching effect, we studied the quenching of emission intensity of **NDI-Ph** and **NDI-Ac-Ph** by increasing **Ph-Vz** concentration in a mixed solution (supporting Information, Figure S28 and S29). The results show that the intermolecular quenching is much less efficient than the quenching observed in the dyads.

The singlet oxygen quantum yields ( $\Phi_{\Delta}$ ) of NDI-Vz dyads and of the reference compounds were measured using 1,3-diphenylisobenzofuran (DPBF) as a  $^1\text{O}_2$  scavenger (Table 1). For **NDI-Ph** and **NDI-Ac-Ph**,  $\Phi_{\Delta} = 18\%$  and  $12\%$  were observed, respectively (in toluene). The ISC is assumed due to the spin orbital coupling effect of the NDI chromophore. For the reference compounds  $\Phi_{\Delta}$  was almost same in solvents with different polarity (*n*-hexane, toluene and acetonitrile). For **NDI-Ph-Vz**,  $\Phi_{\Delta} = 26\%$  in toluene. However, in  $\text{CH}_3\text{CN}$   $\Phi_{\Delta}$  decreases to 2% and in *n*-hexane no singlet oxygen production was observed. For **NDI-Ac-Ph-Vz**,  $\Phi_{\Delta} = 24\%$  in toluene, which is almost two-fold of **NDI-Ac-Ph**. However, in acetonitrile this value decreased to 6%. No singlet oxygen photosensitizing was observed for NDI-

verdazyl dyads in *n*-hexane, which is an evidence for the charge recombination induced ISC (see later section). The singlet oxygen quantum yield is dependent on solvent polarity, therefore an ISC mechanism other than REISC is possible, because REISC should be not sensitive to solvent polarity. Hence we suggest that the ISC is induced by charge recombination (CR), which is further confirmed by fs TA spectral study (see femtosecond transient absorption spectroscopy section).

### Cyclovoltammetric studies and Gibbs free energy changes

The electrochemical properties of the compounds were investigated by cyclovoltammetry (CV) (Figure 4). **NDI-Ph** gives a reversible oxidation wave at +1.15 V and two reversible reduction waves at  $-1.66$  V and  $-1.75$  V, respectively. **Ph-Vz** gives a reversible oxidation peak at +0.48 V and a reversible reduction peak at  $-1.05$  V. It is clear that radical unit is easier to be oxidized as compared to the NDI chromophore. **NDI-Ph-Vz** gives a reversible oxidation peak at +0.48 V and three reversible reduction peaks at  $-1.04$  V,  $-1.34$  V and  $-1.77$  V, respectively. The only oxidation peak in **NDI-Ph-Vz** is assigned to the verdazyl moiety and reduction peak at  $-1.34$  V is associated to the NDI. From these results, it is clear that in the dyads the verdazyl moiety is the electron donor and NDI the electron acceptor. The Gibbs free energy changes for charge separation ( $\Delta G^{\circ}_{\text{CS}}$ ) for the photo-induced electron transfer were calculated by Weller's equation (Eq. 1 and Eq. 2).<sup>[35]</sup>

$$\Delta G^{\circ}_{\text{CS}} = e[E_{\text{OX}} - E_{\text{RED}}] - E_{00} + \Delta G_{\text{S}} \quad (1)$$

$$\Delta G_{\text{S}} = -\frac{e^2}{4\pi\epsilon_s\epsilon_0 R_{\text{CC}}} - \frac{e^2}{8\pi\epsilon_0} \left( \frac{1}{R_{\text{D}}} + \frac{1}{R_{\text{A}}} \right) \left( \frac{1}{\epsilon_{\text{REF}}} - \frac{1}{\epsilon_{\text{S}}} \right) \quad (2)$$

where  $\Delta G_{\text{S}}$  represents the static Coulombic energy elaborated by equation 2.  $e$  = electronic charge,  $E_{\text{OX}}$  = half-wave potential of electron donor moiety for oxidation of single electron ( $-1.34$  V),  $E_{\text{RED}}$  = half-wave potential of electron acceptor moiety (0.48 V);  $E_{00}$  = singlet excited state energy level of NDI approximated with the crossing point of the normalized UV-vis absorption

**Table 2.** Electrochemical redox potentials and driving forces of charge separation ( $\Delta G_{CS}^\circ$ ) and and Charge Recombination ( $\Delta G_{CR}^\circ$ )<sup>[a]</sup>

Compounds	$E_{RED}$ (V)	$E_{OX}$ (V)	$\Delta G_{CS}^\circ$ (eV) <sup>[b]</sup>					$\Delta G_{CR}^\circ$ (eV) <sup>[b]</sup>				
			<i>n</i> -hexane	Toluene	CH <sub>2</sub> Cl <sub>2</sub>	CH <sub>3</sub> CN	CH <sub>3</sub> OH	<i>n</i> -hexane	Toluene	CH <sub>2</sub> Cl <sub>2</sub>	CH <sub>3</sub> CN	CH <sub>3</sub> OH
<b>NDI-Ph-Vz</b>	-1.04,-1.34 -1.77	+0.48	0.04,	-0.11	-0.51	-0.62	-0.62	-2.22	-2.08	-1.67	-1.57	-1.56
<b>NDI-Ph</b>	-1.66,-1.75	+1.15	_[c]	_[c]	_[c]	_[c]	_[c]	_[c]	_[c]	_[c]	_[c]	_[c]
<b>Ph-Vz</b>	-1.05	+0.48	_[c]	_[c]	_[c]	_[c]	_[c]	_[c]	_[c]	_[c]	_[c]	_[c]

[a] Cyclic voltammetric measurements were performed in N<sub>2</sub> saturated CH<sub>2</sub>Cl<sub>2</sub> containing and 0.10 M Bu<sub>4</sub>NPF<sub>6</sub> as supporting electrolyte. Working electrode used was glassy carbon electrode and Ag/AgCl as the reference electrode.  $c = 1.0 \times 10^{-4}$  M. [b] Electron transfer with verdazyl unit as donor and NDI as acceptor in **NDI-Ph-Vz**.  $E_{00}$  is approximated with the crossing point of the normalized UV-vis absorption and fluorescence emission spectra of **NDI-Ph-Vz**. [c] Not applicable.

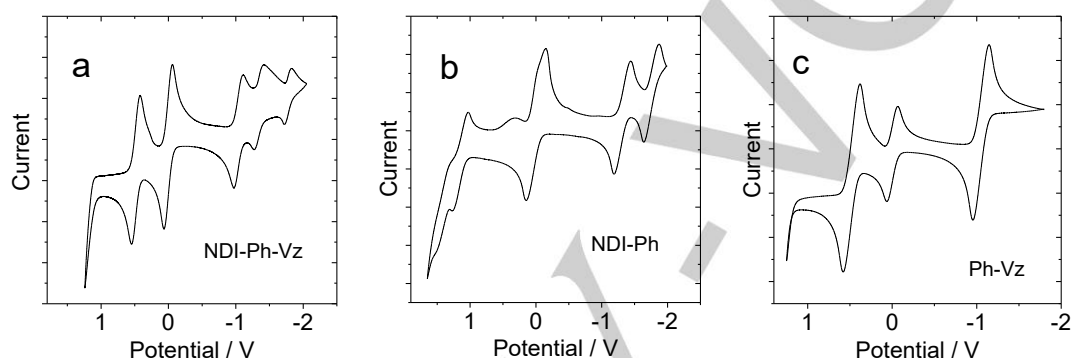


**Figure 4.** Cyclic voltammograms of (a) **NDI-Ph-Vz** (b) **NDI-Ph** and (c) **Ph-Vz**, in deaerated CH<sub>2</sub>Cl<sub>2</sub> with 0.10 M Bu<sub>4</sub>NPF<sub>6</sub> as supporting electrolyte. Internal reference is Ferrocene (Fc/Fc<sup>+</sup>). Scan rate = 0.1 V/s,  $c = 1.0 \times 10^{-4}$  M, 20 °C.

and fluorescence emission, ( $1240/\lambda$ ;  $\lambda = 566$  nm)  $\epsilon_S =$  static dielectric constant of the solvent,  $R_{CC} =$  distance between the centers of electron donor and electron acceptor moiety evaluated by DFT optimized structure,  $R_{CC}$  (**NDI-Ph-Vz**) = 10.95 Å,  $R_D$  represents radius of the electron donor (5.20 Å),  $R_A$  represents the radius of the electron acceptor (5.75 Å),  $\epsilon_{REF}$  is the static dielectric constant of the solvent used for the electrochemical studies,  $\epsilon_0$  is permittivity of free space. The solvents used in the calculations of free energy of the electron transfer are *n*-hexane ( $\epsilon_S = 1.9$ ), toluene ( $\epsilon_S = 2.38$ ), CH<sub>2</sub>Cl<sub>2</sub> ( $\epsilon_S = 9.1$ ), acetonitrile ( $\epsilon_S = 37.5$ ) and methanol ( $\epsilon_S = 32.7$ ).

The value of  $\Delta G_{CS}^\circ$  is positive in *n*-hexane, indicating no electron transfer in this solvent, however, the value is negative in toluene and further higher polarity solvents, indicating that electron transfer is thermodynamically allowed, which was also confirmed by fs TA (for detail see later section). For **NDI-Ac-Ph-Vz**, no CV data were obtained due to its poor solubility.

#### Observation of the triplet excited state with nanosecond transient absorption spectra

In order to verify the formation of triplet states, we measured the nanosecond transient absorption (ns TA) spectra (Figure 5 and 6). NDI without core substitution was reported to possess triplet state formation ability.<sup>[37]</sup> In order to study the ISC of the NDI moiety, we also recorded the ns TA of the references **NDI-Ph**, and **Br-NDI** (Figure 5c and 5f; Supporting Information, Figure S30). Ground state bleaching (GSB) bands centered at 535 nm

and 530 nm were observed for **NDI-Ph** and **Br-NDI**, respectively. For **NDI-Ph** and **Br-NDI**, excited state absorption (ESA) bands were observed in the 330–500 nm and 550–780 nm range. These ESA bands are characteristics for the  $T_1 \rightarrow T_n$  transition of the NDI moiety.<sup>[38, 39]</sup> The triplet state lifetimes of **NDI-Ph** was determined as 114.2 μs, and the decay of the triplet state signal is *mono-exponential*. No TA signals are observed for **NDI-Ph** in aerated solution. In **Br-NDI**, ISC is due to heavy atom effect of Br atom.

The ns TA spectra of **NDI-Ph-Vz** show a GSB band at 535 nm and two ESA bands at 380–510 nm and 555–750 nm (Figure 5a). The comparison with the spectra of the reference compounds indicates that the ESA bands are due to the  $T_1 \rightarrow T_n$  transition of the NDI moiety. The ns TA signals were also observed in aerated solution, however, the intensity was reduced to half (Figure 5b). By monitoring the decay of the transient signal at 440 nm (Figure 5d), a distinct *biexponential* decay was observed, which can be fitted with a component with shorter lifetime of 0.06 μs (81 % Figure 5d) and a component with a long lifetime of 1.9 μs (19 % in population). In aerated solution, **NDI-Ph-Vz** shows a fast decay ( $\tau = 208$  ns, Figure 5e). In order to rule out the scattered light and fluorescence contribution for the short-lived component, the decay curve was compared with instrument response function (IRF).

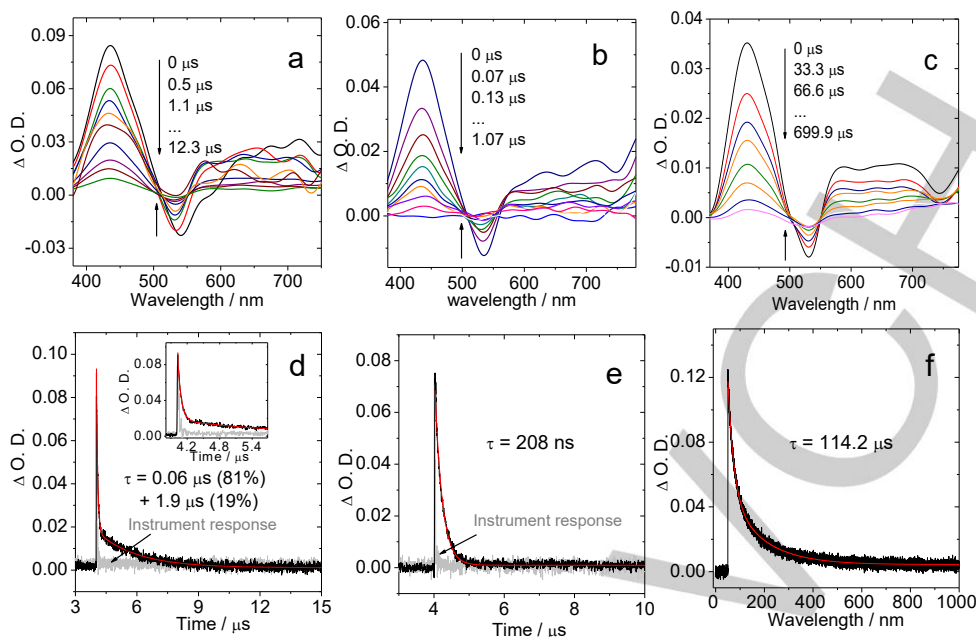


**Figure 5.** Nanosecond time-resolved transient difference absorption spectra of **NDI-Ph-Vz** (a) in deaerated (b) in air saturated solution and (c) **NDI-Ph** in deaerated solution. The decay traces of the **NDI-Ph-Vz** at 440 nm in the (d)  $N_2$  and (e) air saturated solutions and (f) **NDI-Ph** at 440 nm in deaerated solution. Upon nanosecond pulsed laser excitation ( $\lambda_{\text{ex}} = 532$  nm).  $c = 2.0 \times 10^{-5}$  M in toluene, 20 °C. The inset in (d) is the magnifying of the early delay time region to show the difference between the instrument response function (IRF) curve and the decay curve of the transient species.

The ns TA spectra of **NDI-Ph-Vz** are very similar to **NDI-Ac-Ph-Vz** (Figure 6). A GSB band at 550 nm and two ESA bands in the region of 385–510 nm and 580–750 nm were observed. The ESA bands are assigned to the  $T_1 \rightarrow T_n$  transition of NDI moiety. In aerated solvents, the intensity of the TA signals reduces and the lifetime shortens from 2.5  $\mu\text{s}$  to 0.3  $\mu\text{s}$  (Figure 6e). No change was observed for the shorter-lived component (50 ns in deaerated solution and 40 ns in aerated solution). Figure 6d and 6e). In order to rule out the possibility of scattered light, instrument response function was also monitored during ns TA measurement.

Based on the femtosecond transient absorption spectral studies (see later section), we propose that for radical/chromophore dyads, there is electron transfer from verdazyl to NDI followed by charge recombination (CR)-induced ISC. Consequently, the NDI is in its electronic triplet state, and, interacting with the attached verdazyl radical allows for two spin configurations for the whole spin system, namely a doublet (total electron spin quantum number  $S = 1/2$ ) or quartet state ( $S = 3/2$ ), depending on the spin alignment of the three unpaired electrons. We thus attribute the bi-exponential decay of the transient absorption signals to the different lifetimes of the *doublet* and *quartet* states, and we tentatively assign the fast decay component to the  $D_1 \rightarrow D_0$  transition, and the slow-decay component to the  $Q_1 \rightarrow D_0$  transitions. Indeed the former is spin-allowed transition and the latter an ISC process, which is expected to be slower. To the best of our knowledge, this is the first time that the different decay kinetics of the  $D_1$  and the  $Q_1$  states of a radical-chromophore molecular system is directly confirmed with nanosecond transient absorption spectroscopy. In almost all the previously reported multi-spin systems, the lifetime

of the triplet excited state of the chromophore was not determined with ns TA spectroscopy.

Previously, different decay kinetics were observed for the  $D_1$  and  $Q_1$  states of a nitronyl nitroxide radical labeled zinc porphyrin with TREPR,<sup>[40]</sup> but the exact lifetimes of these two state was not determined by ns TA spectra,<sup>[41]</sup> and normally only the high spin state can be observed with TREPR.<sup>[42]</sup> Moreover, the decay kinetics monitored with TREPR may be complicated by the fast spin-lattice-relaxation (SLR).

The  $D_1$  state of a nitroxide radical labeled perylenebisimide (PBI) dyad decays within 46 ns,<sup>[23]</sup> the lifetime of the  $Q_1$  state of this system was determined as ca. 500 ns.<sup>[23]</sup> However, the contribution from electron spin polarization cannot be excluded completely and in the evolution of TREPR signals. Our observations are similar, but ns TA spectroscopy offers a direct and more reliable method to determine the lifetimes of the  $D_1$  and  $Q_1$  states. For instances, a compact NO radical labeled perylene dyad was reported, for which the triplet state of the perylene unit was observed with fs TA spectroscopy, but the triplet state lifetime was not exactly determined.<sup>[18]</sup> In some cases, only the high spin state (for instance quartet or quintet state) but no doublet state ( $D_1$  state) was observed.<sup>[43–44]</sup> The observed lifetime of the triplet state of the NDI unit in the current dyads is much shorter than the intrinsic triplet state lifetime of the NDI chromophore (ca. 32 ~ 276  $\mu\text{s}$ ),<sup>[38,39,45]</sup> which is reasonable because the triplet state localized on the NDI can be quenched by the stable radical.<sup>[23,26,46]</sup> This is also proved by measuring the ns TA spectra of **NDI-Ph** with increasing concentration of **Ph-Vz** (Supporting Information; Figure S31). We observed that with the increasing concentration of **Ph-Vz** the triplet lifetime of **NDI-Ph** decreased from 114.2  $\mu\text{s}$  to 40.2  $\mu\text{s}$ .

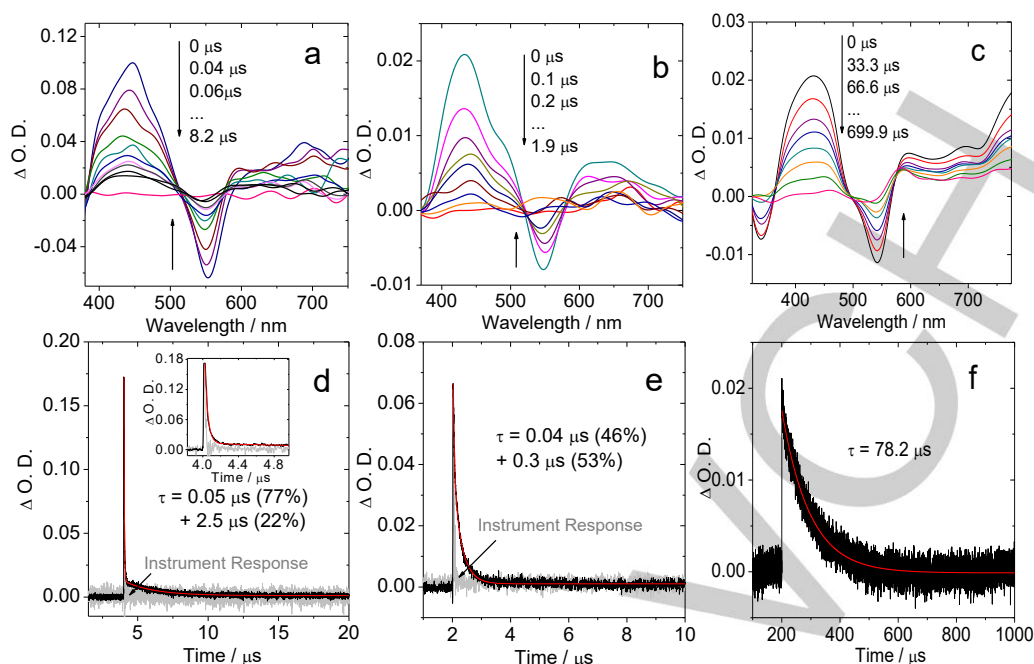


**Figure 6.** Nanosecond transient absorption spectra of **NDI-Ac-Ph-Vz** in (a) deaerated and (b) in air saturated solution. (c) **NDI-Ac-Ph** in deaerated solution. The decay trace of **NDI-Ac-Ph-Vz** at 445 nm (d) in  $N_2$  (e) in air saturated solution (f) **NDI-Ac-Ph** in  $N_2$ , upon ns pulsed laser excitation ( $\lambda_{ex} = 532$  nm).  $c = 2.0 \times 10^{-5}$  M in toluene, 20 °C. The inset in (d) is the magnifying of the early delay time region to show the difference between the instrument response function (IRF) curve and the decay curve of the transient species.

### Femtosecond transient absorption spectroscopy

In order to determine the kinetics of NDI triplet formation, we measured the femtosecond transient absorption spectra of **NDI-Ph-Vz** and **NDI-Ac-Ph-Vz** (Figure 7). It was shown that in radical labeled molecular systems, ISC can be extremely fast. For instance, in a nitroxide-PBI compound, the ISC takes place in ca. 2–3 ps,<sup>[23]</sup> in a TEMPO radical labeled PBI the ISC time constant is ca. 45 ps,<sup>[47]</sup> and in a compact nitroxide radical labeled perylene compound the EISC takes place in 1 ps.<sup>[19]</sup> In a nitroxide radical labeled NDI, the ISC takes ca. 338 ps.<sup>[17]</sup> In a Bodipy-Anthracene-verdazyl triad, charge separation occurs within 120 ps upon photoexcitation.<sup>[48]</sup>

We measured the fs-TA spectra of the reference compounds (Supporting Information; Figure S32–S34). ISC occurred on a timescale longer than 1.5 ns (the maximum pump-probe delay accessible with our system). Only for **Br-NDI** the characteristic spectral signatures of the NDI triplet were observed to rise on a ca. 750 ps timescale (Supporting information, Figure S34).

The kinetic traces recorded for both **NDI-Ph-Vz** and **NDI-Ac-Ph-Vz** were fitted using a global analysis, employing a linear decay scheme with increasing lifetimes and three kinetic components.<sup>[49,50]</sup> Figure 7 shows the Evolution Associated Difference Spectra (EADS) obtained from the analysis of the transient data measured for **NDI-Ph-Vz** and **NDI-Ac-Ph-Vz** in deaerated toluene, upon excitation at 530 nm.

In case of **NDI-Ac-Ph-Vz** (Figure 7a), the transient spectra at early delay times show a GSB band centered at 550 nm and two ESA bands centered at 500 and 650 nm, respectively. These spectral signatures closely resemble to those of the radical anion ( $NDI^{\cdot-}$ ) of **NDI-Ac-Ph-Vz** produced by photoreduction in the presence of TEOA (see later section for detail), and are thus

indicative of the occurrence of ultrafast charge separation (<150 fs, occurring beyond the time resolution of our setup). Features of the verdazyl cation were not observed, possibly due to the low absorption cross section of this species in the visible spectral range. The transient spectra of **NDI-Ac-Ph-Vz** evolves to the second spectrum in 1.4 ps (Figure 7a). The ESA band centered at 650 nm decreases and significantly broadens on its red side. The other ESA blue shifts to 480 nm and decreases in intensity. This spectral component shows signatures similar to those of the NDI triplet, characterized by two ESA bands in the 385–510 nm and 580–750 nm regions (Figure 6). The transient spectrum of **NDI-Ac-Ph-Vz** does not show significant evolution up to the ns timescale, besides a slight decrease observed when going from the second to the third spectral component, on the 187.4 ps timescale, which could be attributed to the vibrational relaxation of the triplet state. The lifetime of the last spectral component (fitted as 12.6 ns) is well beyond the maximum pump-probe delay accessible with our setup, but is well determined by the ns TA measurements reported in the previous section.

The time evolution of the transient spectra is very similar for **NDI-Ph-Vz** (Figure 7b). The only difference is a slight decrease of the ISC rate (1.85 ps, Figure 7b, 7c). Also in this case we observe a relaxation of the triplet state, in 28.8 ps and a long living component, whose exact lifetime exceed the measured timescale of the setup.

In both dyads (**NDI-Ac-Ph-Vz** and **NDI-Ph-Vz**) two phenomenon i.e. charge recombination and ISC are interconnected because the decay of one species is associated with the rise of the second species. Hence we propose that ISC in these dyads is due to CR, not to the initially anticipated REISC.

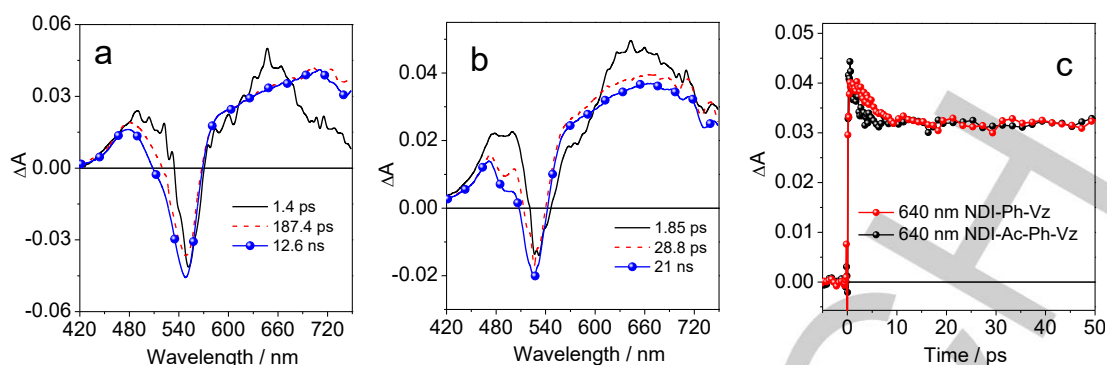


**Figure 7.** EADS (Evolution Associated Difference Spectra) obtained from global analysis of fs-TA data recorded for (a) **NDI-Ac-Ph-Vz** and (b) **NDI-Ph-Vz** in deaerated toluene. (c) Comparison of the kinetic traces at 640 nm for **NDI-Ac-Ph-Vz** and **NDI-Ph-Vz**.

Transient absorption measurements for both dyads were also repeated in acetonitrile (Supporting information; Figure S35). While in case of **NDI-Ac-Ph-Vz** the appearance and evolution of the transient signals showed no significant difference compared with toluene, appreciable difference can be observed for **NDI-Ph-Vz**. For this system indeed spectral signatures characteristic of the NDI anion are observed at early times, but no signatures of ISC could be detected at longer timescale. The spectral evolution can be interpreted in terms of a stabilization of the CS state, which, in polar solvents, lives longer than the time scale investigated with our measurements.

#### Intramolecular spin alignment on the ground state and the excited quartet state

The CW-EPR spectra of the compounds are presented in Figure 8. The  $g$  factor of **NDI-Ph-Vz** ( $g = 2.0046$ ) and **NDI-Ac-Ph-Vz** ( $g = 2.0034$ ) are very close to that of **Ph-Vz** ( $g = 2.0038$ ).

The photophysical properties of the NDI-radical dyads were also investigated using theoretical computations (DFT) with two basis sets B3LYP/6-31G(d) and B3LYP/6-31G+(d) (Table 3; Supporting Information, Figure S37 ~ S40; Table S2 ~ S4). Negligible difference of molecular orbitals was observed for two different basis sets. To better clarify the spin-spin interaction between the radical and the NDI chromophore we resorted to theoretical computations.

At the  $D_0$  state, the dihedral angle between the NDI and the phenyl ring attached to the verdazyl unit is  $60.7^\circ$ , and it reduces to  $43.8^\circ$  at the  $Q_1$  state for **NDI-Ph-Vz** (Figure 9). For **NDI-Ac-Ph-Vz**, the difference in dihedral angles between the  $D_0$  and  $Q_1$  states is not significant. For **NDI-Ac-Ph-Vz**, the two moieties are coplanar in both the  $D_0$  and  $Q_1$  states (the torsion is  $0.5 \sim 0.6^\circ$ ), which indicates the occurrence of significant  $\pi$ -conjugation between the units. The spin density surfaces of the dyads at the  $D_0$  state and the  $Q_1$  state were also computed. The spin density of the  $D_0$  state of **NDI-Ph-Vz** is localized on radical part (Figure 10a). However, there is a spin leakage towards the phenyl linker between the oxoverdazyl and the NDI units. For the quartet state, the spin density surface is localized on the entire molecule. Similar results were observed for **NDI-Ac-Ph-Vz** (Supporting Information, Figure S36).

Based on the energy levels of the  $D_1$  and the  $Q_1$  states of **NDI-Ph-Vz**, we propose that the interaction between the radical

(in doublet state) and the NDI chromophore (in triplet state) is *ferromagnetic*, i.e.  $J > 0$  and the  $D_1$  state has higher energy than the  $Q_1$  state (Table 3. Supporting Information, Figure S37). Direct determination of the magnitude of the spin exchange coupling of the radical with the chromophore at the excited state is impossible, although the relative energy of the  $D_1$  and  $Q_1$  state can be derived from electron spin polarization dynamics.<sup>[23]</sup> The occurrence of  $\pi$ -conjugation between the radical and the chromophore may increase the exchange magnitude,<sup>[27]</sup> thus our calculated  $J = 0.07$  eV ( $564$   $\text{cm}^{-1}$ ) is reasonable. For **NDI-Ac-Ph-Vz** the calculated  $J = 0.13$  eV ( $1048$   $\text{cm}^{-1}$ ) is slightly higher than **NDI-Ph-Vz** (Supporting Information, Figure S39). The formation of  $D_1$  and  $Q_1$  states is supported by the biexponential decay of the triplet states of the radical dyads.

The photophysics of the compounds can be summarized in Scheme 2. Upon photoexcitation of **NDI-Ph-Vz**, ultrafast electron transfer takes place ( $<150$  fs; beyond the time resolution of our instrument) from verdazyl to NDI, followed by charge recombination, which leads to the formation of the triplet state of NDI (1.85 ps) as confirmed by fs TA spectra and singlet oxygen photosensitizing. This triplet state interacts with the unpaired electron of the verdazyl and produce quartet and doublet states, as supported by ns TA spectra. Similar phenomena also take place in **NDI-Ac-Ph-Vz**. Electron transfer occurs beyond the instrument resolution and charge recombination ISC takes place in about 1.4 ps (slightly faster than **NDI-Ph-Vz**). The triplet state of the NDI moiety, by spin-spin exchange with verdazyl radical, forms excited doublet ( $D_1$ ) and quartet ( $Q_1$ ) state. Note that for both the  $D_1$  and  $Q_1$  state, the NDI moiety is in triplet state. The ns TA spectra confirm that the fast-decaying component is more abundant than the slow-decaying component (Figure 5 and 6). ISC is induced by CR shown by the fs TA spectral study, ISC is solvent polarity dependent.

Our DFT computations shown that the spin-spin exchange between the radical and the NDI moiety is *ferromagnetic*, thus the  $Q_1$  state has lower energy than the  $D_1$  state. Similar results were also observed for **NDI-Ac-Ph-Vz**. The decay of the  $D_1$  state to the ground state ( $D_0$ ), is spin allowed, i.e.  $D_1 \rightarrow D_0$  can be considered as an internal conversion, although the NDI moiety is in a triplet state. The decay of the  $Q_1$  state to the ground state is more spin-forbidden, therefore we expect a longer lifetime for the  $Q_1$  state compared to the  $D_1$  state. Indeed, we observed a

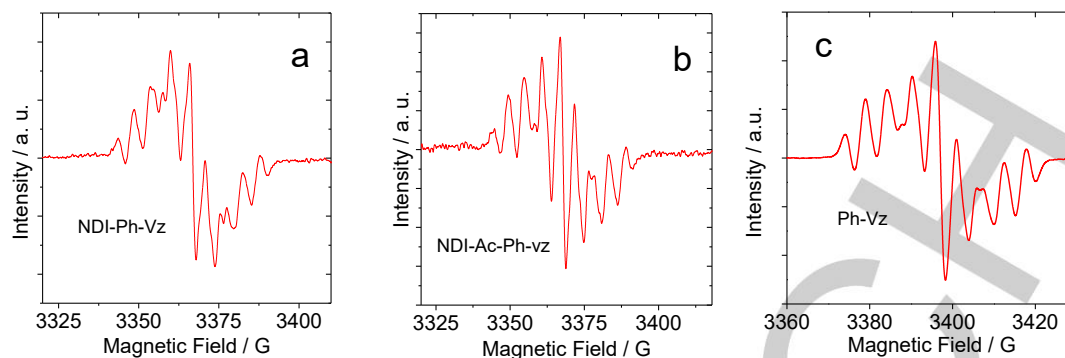


**Figure 8.** ESR spectra of (a) **NDI-Ph-Vz**, (b) **NDI-Ac-Ph-Vz** and (c) **Ph-Vz** in deaerated  $\text{CH}_2\text{Cl}_2$ .  $c = \text{ca. } 1.0 \times 10^{-4} \text{ M}$ ,  $20^\circ\text{C}$ .

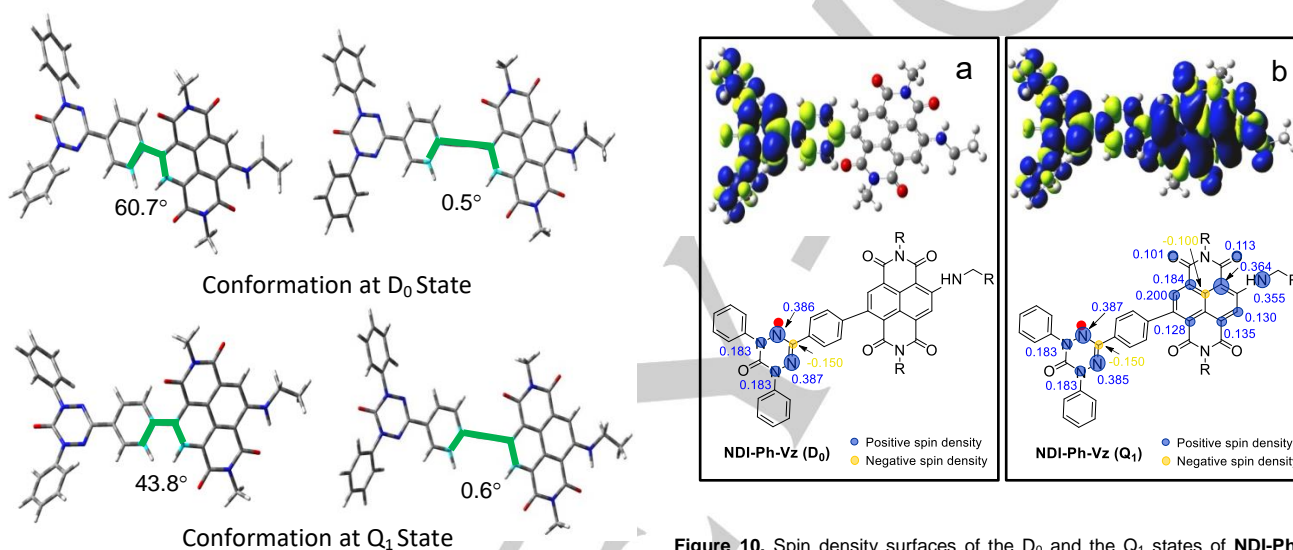


**Figure 9.** Optimized conformations (energy minimized) and the dihedral angles of the selected atoms in **NDI-Ph-Vz** (left) and **NDI-Ac-Ph-Vz** (right) at the  $D_0$  and  $Q_1$  states, calculated by UB3LYP/6-31G (d) level using Gaussian 09W.

*biexponential* decay for the triplet state lifetime monitored by nanosecond transient absorption spectroscopy. To the best of our knowledge, this is the first time that the different decay kinetics of the  $D_1$  and  $Q_1$  states were observed by ns TA spectroscopy.

#### Photo-driven intermolecular electron transfer: Photoreduction to produce NDI radical anion

Photo-driven intermolecular electron transfer is a primary process involved in the photo-redox catalytic reactions in organic chemistry.<sup>[51,52]</sup> We studied the formation of the radical anion of NDI through photosensitization of our compounds (**NDI-Ph-Vz** and **NDI-Ac-Ph-Vz**) in the presence of sacrificial electron donor triethanolamine (TEOA) (Figure 11).

Conversion of NDI into its radical anion was achieved by chemical sensitization method, for example in the presence of cyanide anion,<sup>[53]</sup> however, photosensitization methods to

**Figure 10.** Spin density surfaces of the  $D_0$  and the  $Q_1$  states of **NDI-Ph-Vz** calculated at UB3LYP/6-31G (d) level using Gaussian 09W. (a)  $D_0$  state (b)  $Q_1$  state. Alkyl chains are replaced by methyl/ethyl groups to reduce calculation time. The spin density of atoms with negligible values is not presented.

generate the radical anion of NDI are rarely reported. UV-vis absorbance of **NDI-Ph-Vz** was observed at 297, 370, 533 and 580 nm. Although no change in absorbance was initially observed upon the addition of TEOA (Figure 11a), when the mixture of **NDI-Ph-Vz** and TEOA was irradiated with a 35 W Xe lamp for 4 minutes, the color of solution changed from light pink to salmon-orange (Figure 11b). The photoirradiated solution shows new absorption bands centered at 494, 620, 750 and 835 nm. These new absorbance bands are similar to those previously reported for  $\text{NDI}^{\cdot-}$ , produced by reduction of NDI in the presence of cyanide anion.<sup>[53]</sup> When the photo-irradiated mixture was exposed to air, the  $\text{NDI}^{\cdot-}$  was oxidized to its neutral form, as confirmed by UV-vis absorption. (Figure 11a and 11b). We investigated the reversibility of NDI photoreduction for five cycles, only a very minor decomposition was observed (Figure 11c). Similarly, the radical anion of **NDI-Ac-Ph-Vz** can be also generated by photosensitization method in the presence of TEOA (Supporting Information, Figure S43). The photo-driven electron transfer properties of these NDI dyads make these compounds potential candidates for photocatalysis, for instance in applications devoted to split water for the production of  $\text{H}_2$ .

**Table 3.** Electronic excitation energies (eV) and corresponding oscillator strengths ( $f$ ), main configurations, and CI coefficients of the low-lying excited states of **NDI-Ph-Vz**, calculated by TDDFT//UB3LYP/6-31G(d), based on the optimized ground state geometries. Toluene is used as solvent in the calculations.

Electronic Transitions	TDDFT// UB3LYP/6-31G(d)				
	Energy [a]	$f$ [b]	Composition [c]	CI [d]	$\langle S^2 \rangle$ [e]
$D_0 \rightarrow Q_1$	1.67 eV / 743 nm	0.0000	H-1 $\alpha$ $\rightarrow$ L $\alpha$	0.6818	2.77
$D_0 \rightarrow D_1$	1.89 eV / 656 nm	0.0001	H $\alpha$ $\rightarrow$ L $\alpha$	0.9924	0.82
$D_0 \rightarrow D_2$	2.26 eV / 549 nm	0.0542	H-1 $\beta$ $\rightarrow$ L $\beta$	0.6976	0.76
			H $\alpha$ $\rightarrow$ L+1 $\alpha$	0.1823	
$D_0 \rightarrow D_3$	2.39 eV / 518 nm	0.0935	H-1 $\beta$ $\rightarrow$ S $\beta$	0.5281	2.00
$D_0 \rightarrow D_4$	2.40 eV / 517 nm	0.1280	H-1 $\beta$ $\rightarrow$ S $\beta$	0.5221	1.73
			H-1 $\beta$ $\rightarrow$ L $\beta$	0.5101	
$D_0 \rightarrow D_5$	3.69 eV / 336 nm	0.1388	H $\alpha$ $\rightarrow$ L+4 $\alpha$	0.4492	1.66

[a] Only the selected low-lying excited states are presented. [b] Oscillator strength. [c] H stands for HOMO (i.e. SOMO for the radical compound), L stands for LUMO. Only the main configurations are presented. [d] The CI coefficients are in absolute values. [e] Spin angular momentum. Theoretical values of  $S^2$  for doublet and quartet are 0.75 and 3.75 respectively.

## Conclusions

We connected a verdazyl radical moiety with naphthalenediimide (NDI) via two different linkers, i.e. phenyl or ethynylphenyl, to prepare two different NDI-Vz dyads and study the effect of radical on the photophysical properties, especially the radical enhanced intersystem crossing (REISC). With steady state and nanosecond/femtosecond time-resolved transient absorption spectroscopies, as well as DFT computations, we show that the fluorescence quantum yield decreased significantly from the reference NDI chromophores (29% ~ 80%) to the radical compounds (0.3% ~ 0.7%), depend on the linker in the dyads. Femtosecond transient absorption spectroscopy demonstrated that ultrafast charge separation (<150 fs) occurred upon photoexcitation, followed by charge recombination-induced ISC (1.40 ps ~ 1.85 ps). ISC in these dyads occurs on a much faster timescale than the intrinsic ISC of the NDI chromophore without radical moiety (1.5 ns). The charge recombination induced ISC was also supported by the solvent polarity-dependency of the singlet oxygen quantum yields ( $\Phi_{\Delta}$ ) of the radical dyads. In *n*-hexane where electron transfer is thermodynamically not allowed, no ISC was observed, in toluene the  $\Phi_{\Delta}$  is up to 26%. We propose the triplet state on the chromophore may interact with the doublet state of verdazyl and hence doublet ( $D_1$ . Total spin quantum number  $S = 1/2$ ) and

quartet state ( $Q_1$ . Total spin quantum number  $S = 1/2$ ) are formed. This is supported by the observation of a distinct biexponential decay of the  $T_1$  state in the dyads by nanosecond transient absorption spectroscopy. The fast-decaying component (50 ns, population ratio: 80%) is attributed to the spin allowed  $D_1 \rightarrow D_0$  internal conversion, and the slow-decaying component (2  $\mu$ s, population ratio: 20%) is assigned to the  $Q_1 \rightarrow D_0$  ISC. DFT computations reconstructed the energy diagrams suggesting the occurrence of ferromagnetic interactions between the radical and the triplet localized on the NDI moiety, which are predicted  $J = 0.07$  eV and  $J = 0.13$  eV for the dyads, respectively (dyad with ethynyl linker gives stronger interaction). Photo-driven intermolecular electron transfer between the radical dyads and sacrificial electron donor was achieved, demonstrated by the formation of the NDI radical anion its oxidation to the neutral form by exposure of the photo-irradiated solution to air. These results are useful for studying the spin dynamics of radical labeled visible light-harvesting organic chromophores, as well as for preparation of the heavy atom-free triplet photosensitizers.

## Experimental Section

### General procedures

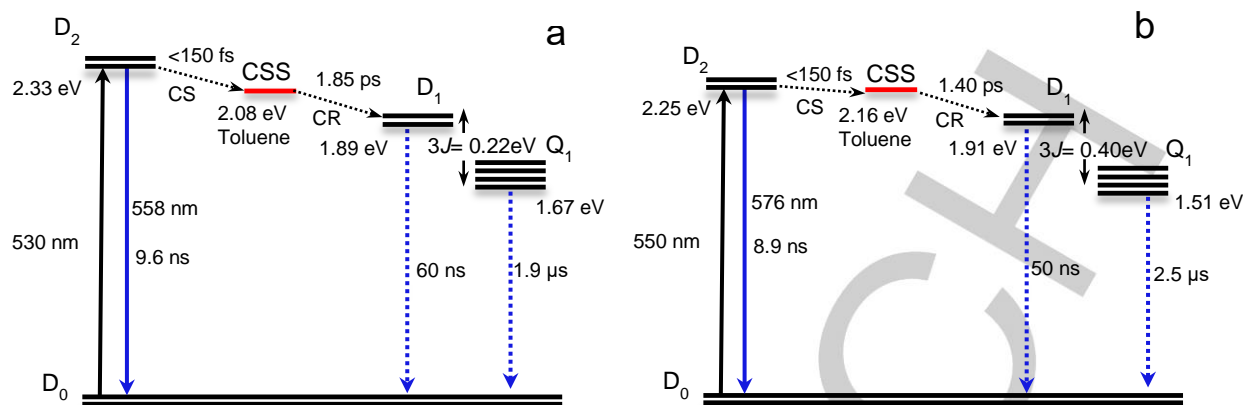
Analytically pure compounds, as received from the supplier were used to synthesize all the compounds. Fluorescence lifetimes of compounds were monitored by OB920 luminescence lifetime spectrometer (Edinburgh Instruments, UK). RF5301 PC spectrofluorometer (Shimadzu Ltd., Japan) was used to record fluorescence spectra. For all the measurements in deaerated solvents, the sample was purged with inert gas for 15 minutes prior to the measurement.

### General procedures

Synthesis of **Br-NDI**, **NDI-Ph**, compounds **1-8** are presented in the Supporting Information.

**Synthesis of the compound NDI-Ph-Vz:** Br-NDI (70 mg, 0.1 mmol) and compound **5** (35 mg, 0.1 mmol) were dissolved in dry toluene (8 mL). Diisopropylamine (0.5 mL) and Pd(PPh<sub>3</sub>)<sub>4</sub> (25 mg, 0.02 mmol) was added to this mixture under Ar atmosphere and the mixture was allowed to be stirred at 80 °C for 18 h. After drying the solvent under reduced pressure, the crude product was purified by column chromatography (silica gel; CH<sub>2</sub>Cl<sub>2</sub>). The product was obtained as dark brown powder (Yield: 50 mg, 51 %). Due to the presence of the paramagnetic radical moiety in the molecule, no satisfactory <sup>1</sup>H NMR spectrum can be obtained. FT-IR (KBr): 3420, 2958, 2925, 2855, 1728, 1681, 1636, 1582, 1436, 1382, 1265, 1196, 1132, 1076, 879, 795, 744, 693, 632, 516 cm<sup>-1</sup>. TOF MALDI-HRMS ([C<sub>60</sub>H<sub>68</sub>N<sub>7</sub>O<sub>5</sub>]<sup>+</sup>) Calcd:  $m/z = 967.5360$  for [M+H]<sup>+</sup>. Found:  $m/z = 967.5336$ . Anal. Calcd for [C<sub>60</sub>H<sub>68</sub>N<sub>7</sub>O<sub>5</sub> + 0.15CH<sub>2</sub>Cl<sub>2</sub>]: C, 73.72; H, 7.03; N, 10.01. Found: C, 73.82; H, 7.05; N, 9.90.

**Synthesis of the compound NDI-Ph-Vz:** Compound **8** (45 mg, 0.1 mmol) and **Br-NDI** (70 mg, 0.1 mmol) were dissolved in acetone/water (3 mL, 2:1, v/v). K<sub>2</sub>CO<sub>3</sub> (34 mg, 0.25 mmol) and Pd(OAc)<sub>2</sub> (2 mg, 0.01 mmol) was added under Ar atmosphere and the reaction was stirred at



**Scheme 2.** Energy Diagram Showing the Photophysical Properties of the (a) **NDI-Ph-Vz** and (b) **NDI-Ac-Ph-Vz**, upon Photoexcitation.  $D$  stands for Doublet States;  $Q$  stands for quartet state. Ferromagnetic coupling ( $J > 0$ ) exists between the radical and the electronically excited NDI unit.

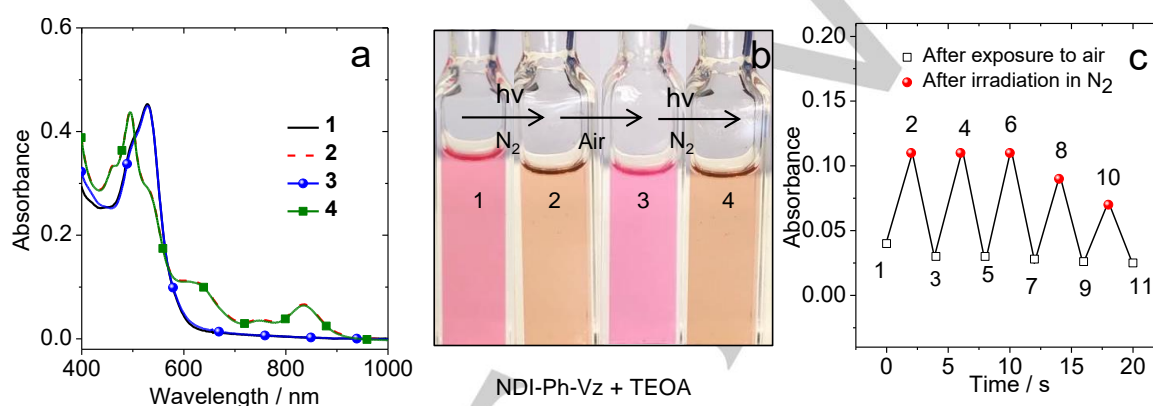


**Figure 11.** Reversible photoreduction of the dyad. (a) **NDI-Ph-Vz**; Reversibility of UV-vis absorption spectra, (1) **NDI-Ph-Vz** + TEOA in aerated solution; (2) **NDI-Ph-Vz** + TEOA in deaerated solution irradiated for 2 minutes; (3) **NDI-Ph-Vz** + TEOA exposed to air; (4) **NDI-Ph-Vz** + TEOA in  $N_2$  re-irradiated for 2 minutes. (b) Photographs showing the reversibility the changes of the solutions in (a). (c) The reversibility of the formation of radical anion of NDI shown by **NDI-Ph-Vz**. With absorption at 607 nm. The photo-irradiation was performed with a 35 W xenon lamp, at power density = 55.0 mW/cm<sup>2</sup>.  $c(\text{NDI-Ph-Vz}) = 2.0 \times 10^{-5}$  M,  $c(\text{TEOA}) = 2.0 \times 10^{-2}$  M, in  $\text{CH}_3\text{CN}$ , 20 °C.

60 °C for 2 h. After completion of reaction, the crude mixture was dried and added to water. The mixture was extracted with DCM (3 × 100 mL), concentrated under reduced pressure and purified by column chromatography (silica gel;  $\text{CH}_2\text{Cl}_2$ ). The product was obtained as dark brown powder (Yield: 40 mg, 43 %). Due to the presence of the paramagnetic radical moiety in the molecule, no satisfactory <sup>1</sup>H NMR spectrum can be obtained. FT-IR (KBr): 3421, 2957, 2920, 2852, 1926, 1703, 1639, 1611, 1456, 1359, 1270, 1195, 1132, 1077, 878, 752, 690, 665, 631 cm<sup>-1</sup>. TOF MALDI-HRMS ( $[\text{C}_{58}\text{H}_{68}\text{N}_7\text{O}_5]^+$ ) Calcd:  $m/z = 942.5282$ . Found:  $m/z = 942.5269$ . Anal. Calcd for  $[\text{C}_{58}\text{H}_{68}\text{N}_7\text{O}_5^+ + 0.6\text{CH}_2\text{Cl}_2]$ : C, 70.80; H, 7.02; N, 9.86. Found: C, 71.10; H, 7.26; N, 10.00.

**Nanosecond Transient Absorption Spectroscopy.** The samples for nanosecond transient absorption (ns TA) studies were analysed by LP980 laser flash-photolysis spectrometer (Edinburgh Instrument, UK) and oscilloscope (Tektronix TDS 3012B) was used to digitized the transient signals. The data was analysed by L900 software. The samples were purged with  $N_2$  for 15 minutes prior to measurement.

**Femtosecond transient absorption spectra.** The apparatus used for the sub-picosecond transient absorption spectroscopy (TAS) measurements is based on a Ti:sapphire regenerative amplifier (BMI Alpha 1000) system pumped by a Ti:sapphire oscillator (Spectra Physics Tsunami). The system produces 100 fs pulses at 785 nm, 1 kHz repetition rate and average power of 450–500 mW. Excitation pulses at 530 nm have been obtained by pumping a home-made non collinear optical parametric amplifier (NOPA) by a portion of the fundamental 785 nm. The pump beam polarization has been set to magic angle with respect to the probe beam by rotating a  $\lambda/2$  plate. Excitation powers were on the order of 30–50 nJ. The probe pulse was generated by focusing a small portion of the fundamental laser output radiation on a 2 mm thick sapphire window. Pump-probe delays were introduced by sending the probe beam through a motorized stage. Multichannel detection was achieved by sending the white light continuum after passing through the sample to a flat field monochromator coupled to a home-made CCD detector [for more information see <http://lens.unifi.it/ew>]. TAS measurements were carried out in a quartz cell (2 mm thick) mounted on a movable stage to avoid sample photo degradation and multiple photon excitation. The recorded kinetic traces and transient spectra have been analysed by using a global analysis.<sup>[49]</sup> The number of kinetic components has been estimated by performing a preliminary singular values decomposition (SVD) analysis.<sup>[54]</sup> Global analysis was performed

using the GLOTARAN package (<http://glotaran.org>),<sup>[50]</sup> and employing a linear unidirectional "sequential" model.

**Density function theory (DFT) computation.** The DFT was used for molecular geometries and spin density surfaces optimization with UB3LYP (for radicals) and B3LYP (for neutral molecules) functional, using 6-31G(d) and 6-31G+(d) basis set. The time dependent TD-DFT was used to calculate excited state energy using UB3LYP/6-31G(d) and UB3LYP/6-31G+(d) level of theory. The sign and the magnitude of the  $3J$  value were approximated from difference of energy between optimized  $D_1$  and  $Q_1$  states. All the geometries are at energy minima and no imaginary frequency was observed for all related calculations. Toluene ( $\epsilon = 2.37$ ) was used as solvent with conductor-like polarizable continuum model (CPCM) for all calculation.<sup>[51]</sup> We used Gaussian 09W for all the calculations.<sup>[34]</sup>

## Acknowledgements

J. Z. thanks the NSFC (21673031, 21761142005, 2181101275 and 21421005) and State Key Laboratory of Fine Chemicals (ZYTS201901) for financial support.

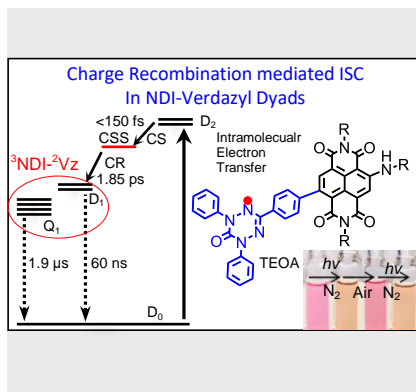
**Keywords:** Intersystem crossing • Electron transfer • Naphthalenediimide • Photocatalysis • Triplet photosensitizer

- [1] A. Kamkaew, S. H. Lim, H. B. Lee, L. V. Kiew, L. Y. Chung, K. Burgess, *Chem. Soc. Rev.* **2013**, *42*, 77–88.
- [2] J. Zhao, W. Wu, J. Sun, S. Guo, Triplet Photosensitizers: From Molecular Design to Applications. *Chem. Soc. Rev.* **2013**, *42*, 5323–5351.
- [3] J. P. Celli, B. Q. Spring, I. Rizvi, C. L. Evans, K. S. Samkoe, S. Verma, B. Pogue, T. Hasan, *Chem. Rev.* **2010**, *110*, 2795–2838.
- [4] P. Majumdar, R. Nomula, J. Zhao, *J. Mater. Chem. C* **2014**, *2*, 5982–5997.
- [5] J. Zhao, K. Xu, W. Yang, Z. Wang, F. Zhong, *Chem. Soc. Rev.* **2015**, *44*, 8904–8939.
- [6] J. Zhao, S. Ji, W. Wu, H. Guo, J. Sun, H. Sun, Y. Liu, Q. Li, L. Huang, *RSC Adv.* **2012**, *2*, 1712–1728.
- [7] Y. You, W. Nam, *Chem. Soc. Rev.* **2012**, *41*, 7061–7084.
- [8] A. Kawai, K. Shibuya, *J. Photochem. Photobiol. C: Photochem. Rev.* **2006**, *7*, 89–103.
- [9] Z. Wang, J. Zhao, A. Barbon, A. Toffoletti, Y. Liu, Y. An, L. Xu, A. Karatay, H. G. Yagliglu, E. A. Yildiz, et al. Radical-Enhanced Intersystem Crossing in New Bodipy Derivatives and Application for Efficient Triplet–Triplet Annihilation Upconversion. *J. Am. Chem. Soc.* **2017**, *139*, 7831–7842.
- [10] H. Yiming, X. Zihao, J. Shijian, L. Chenyang, W. Kurt, E. Francesco, L. Tianquan, E. Elif, *Chem. Mater.* **2018**, *30*, 7840–7851.
- [11] P. Li, T. Xie, X. Duan, F. Yu, X. Wang, B. Tang, *Chem – Eur. J.* **2010**, *16*, 1834–1840.
- [12] G. Likhtenstein, K. Ishii, S. I. Nakatsuji, *Photochem. Photobiol.* **2007**, *83*, 871–881.
- [13] B. K. Hughes, W. A. Braunecker, A. J. Ferguson, T. W. Kemper, R. E. Larsen, T. Gennett, *J. Phys. Chem. B* **2014**, *118*, 12541–12548.
- [14] D. Matuschek, S. Eusterwiemann, L. Stegemann, C. Doerenkamp, B. Wibbeling, C. G. Daniliuc, N. L. Doltsinis, C. A. Strassert, H. Eckert, A. Studer, *Chem. Sci.* **2015**, *6*, 4712–4716.
- [15] N. M. Gallagher, A. Olankitwanit, A. Rajca, *J. Org. Chem.* **2015**, *80*, 1291–1298.
- [16] M. Abe, *Diradicals. Chem. Rev.* **2013**, *113*, 7011–7088.
- [17] Z. Wang, Y. Gao, M. Hussain, S. Kundu, V. Rane, M. Hayvali, E. A. Yildiz, J. Zhao, H. G. Yagliglu, R. Das, L. Luo, *Chem.–Eur. J.* **2018**, *24*, 18663–18675.
- [18] V. Rane, R. Das, *J. Phys. Chem. A* **2015**, *119*, 5515–5523.
- [19] Y. Teki, H. Tamekuni, K. Haruta, J. Takeuchi, Y. Miura, *J. Mater. Chem.* **2008**, *18*, 381–391.
- [20] S. M. Dyar, E. A. Margulies, N. E. Horwitz, K. E. Brown, M. D. Krzyaniak, M. R. Wasielewski, *J. Phys. Chem. B* **2015**, *119*, 13560–13569.
- [21] N. Medvedeva, V. Martin, A. L. Weis, G. I. Likhstenshten, *J. Photochem. Photobiol. A: Chem.* **2004**, *163*, 45–51.
- [22] Y. Teki, M. Kimura, S. Narimatsu, K. Ohara, K. Mukai, *Bull. Chem. Soc. Jpn.* **2004**, *77*, 95–99.
- [23] D. Schmidt, M. Son, J. M. Lim, M. J. Lin, I. Krummenacher, H. Braunschweig, D. Kim, F. Würthner, *Angew. Chem. Int. Ed.* **2015**, *54*, 13980–13984.
- [24] E. M. Giacobbe, Q. Mi, M. T. Colvin, B. Cohen, C. Ramanan, A. M. Scott, S. Yeganeh, T. J. Marks, M. A. Ratner, M. R. Wasielewski, *J. Am. Chem. Soc.* **2009**, *131*, 3700–3712.
- [25] N. J. Turro, M. H. Kleinman, E. Karatekin, *Angew. Chem. Int. Ed.* **2000**, *39*, 4436–4461.
- [26] J. i. Fujisawa, Y. Ohba, S. Yamauchi, *J. Phys. Chem. A* **1997**, *101*, 434–439.
- [27] A. Kawai, K. Obi, *J. Phys. Chem.* **1992**, *96*, 52–56.
- [28] Y. Teki, S. Miyamoto, K. Iimura, M. Nakatsuji, Y. Miura, *J. Am. Chem. Soc.* **2000**, *122*, 984–985.
- [29] A. Ito, N. Kobayashi, Y. Teki, *Inorg. Chem.* **2017**, *56*, 3794–3808.
- [30] E. T. Chernick, R. Casillas, J. Zirzmeier, D. M. Gardner, M. Gruber, H. Kropp, K. Meyer, M. R. Wasielewski, D. M. Guldi, R. Tykwinski, *J. Am. Chem. Soc.* **2015**, *137*, 857–863.
- [31] Y. Teki, S. Miyamoto, M. Nakatsuji, Y. Miura, *J. Am. Chem. Soc.* **2001**, *123*, 294–305.
- [32] E. Terada, T. Okamoto, M. Kozaki, M. E. Masaki, D. Shiomi, K. Sato, T. Takui, K. Okada, *J. Org. Chem.* **2005**, *70*, 10073–10081.
- [33] Y. Teki, T. Toichi, S. Nakajima, *Chem.–Eur. J.* **2006**, *12*, 2329–2336.
- [34] E. Terada, T. Okamoto, M. Kozaki, M. E. Masaki, D. Shiomi, K. Sato, T. Takui, K. Okada, *J. Org. Chem.* **2005**, *70*, 10073–10081.
- [35] M. J. Frisch, G. W. Trucks, H. B. Schlegel, G. E. Scuseria, M. A. Robb, J. R. Cheeseman, G. Scalmani, V. Barone, B. Mennucci, G. A. Petersson, et al. Gaussian 09, Gaussian, Inc.: Wallingford, CT, USA, **2009**.
- [36] R. Ziesel, B. d. Allen, D. B. Rewinska, A. Harriman, *Chem.–Eur. J.* **2009**, *15*, 7382–7393.
- [37] J. W. Shi, M. E. El-Khouly, K. Ohkubo, S. Fukuzumi, *Chem.–Eur. J.* **2013**, *19*, 11332–11341.R.
- [38] P. Ganesan, J. Baggerman, H. Zhang, E. J. R. Sudhölter, H. Zuilhof, *J. Phys. Chem. A* **2007**, *111*, 6151–6156.
- [39] F. Doria, I. Manet, V. Grande, S. Monti, M. Freccero, *J. Org. Chem.* **2013**, *78*, 8065–8073.
- [40] M. Hussain, J. Zhao, W. Yang, F. Zhong, A. Karatay, H. G. Yagliglu, E. A. Yildiz, M. Hayvali, *J. Luminesc.* **2017**, *192*, 211–217.F. J. W. Shi, M. E. El-Khouly, K. Ohkubo, S. Fukuzumi, *Chem.–Eur. J.* **2013**, *19*, 11332–11341.R.
- [41] K. Ishii, J. I. Fujisawa, Y. Ohba, S. A. Yamauchi, *J. Am. Chem. Soc.* **1996**, *118*, 13079–13080.
- [42] J. I. Fujisawa, K. Ishii, Y. Ohba, S. Yamauchi, M. Fuhs, K. Möbius, *J. Phys. Chem. A* **1999**, *103*, 213–216.
- [43] K. Ishii, Y. Hirose, H. Fujitsuka, O. Ito, N. Kobayashi, *J. Am. Chem. Soc.* **2001**, *123*, 702–708.
- [44] Y. Teki, M. Nakatsuji, Y. Miura, *Mol. Phys.* **2002**, *100*, 1385–1394.
- [45] Y. Teki, H. Tamekuni, J. Takeuchi, Y. Miura, *Angew. Chem. Int. Ed.* **2006**, *45*, 4666–4670.
- [46] Y. Liu, W. Wu, J. Zhao, X. Zhang, H. Guo, *Dalton Trans.* **2011**, *40*, 9085–9089.

- [46] S. Jockusch, O. Zeika, N. Jayaraj, V. Ramamurthy, N. J. Turro, *J. Phys. Chem. Lett.* **2010**, *1*, 2628–2632.
- [47] M. T. Colvin, E. M. Giacobbe, B. Cohen, T. Miura, A. M. Scott, M. R. Wasielewski, *J. Phys. Chem. A* **2010**, *114*, 1741–1748.S.
- [48] K. Kanemoto, A. Fukunaga, M. Yasui, D. Kosumi, H. Hashimoto, H. Tamekuni, Y. Kawahara, Y. Takemoto, J. Takeuchi, Y. Miura, et al., *RSC Adv.* **2012**, *2*, 5150–5153.
- [49] J. J. Snellenburg, S. P. Liptonok, R. Seger, K. M. Mullen, I. H. M. J. *Stat. Softw.* **2012**, *49*, 1–22.K.
- [50] I. H. M. Stokkum, D. S. Larsen, R. V. Grondelle, *B. B. A. Bioenerge.* **2004**, *1657*, 82–104.
- [51] Y. Xi, H. Yi, A. Lei, *Org. & Biomol. Chem.* **2013**, *11*, 2387–2403.
- [52] D. P. Hari, B. König, *Chem. Commun.* **2014**, *50*, 6688–6699.
- [53] M. R. Ajayakumar, D. Asthana, P. Mukhopadhyay, *Org. Lett.* **2012**, *14*, 4822–4825.
- [54] E. Henry, J. Hofrichter, *Method. Enzymol.* **1992**, *210*, 129–192.
- [55] M. Cossi, N. Rega, G. Scalmani, V. Barone, *J. Comput. Chem.* **2003**, *24*, 669–681.

## FULL PAPER

We synthesized novel NDI-verdazyl dyads to study the effect of radial on photophysical properties. Fluorescence quenching and ultrafast electron transfer were observed, followed by charge recombination induced intersystem crossing. Spin-spin interaction of the NDI triplet state with verdazyl radical results in doublet ( $D_1$ ) and quartet states ( $Q_1$ ), supported by the distinct biexponential decay kinetics. Reversible formation of radical anion of NDI moiety was achieved by photo-reduction in the presence of sacrificial electron donor.



## ! Photochemistry

Mushraf Hussain, Maria Taddei, Laura Bussotti, Paolo Foggi, Jianzhang Zhao\*  
Qingyun Liu,\* and Mariangela Di Donato\*

Page No. – Page No.

**Intersystem Crossing in  
Naphthalenediimide-Oxoverdazyl  
Dyads: Synthesis and Photophysical  
Studies**